SYNTHESIS AND CHARACTERIZATION OF Ce-DOPED BISMUTH FERRITE

Thesis Submitted in Partial fulfilment of the requirement for

The award of the degree of

Master of Science (M.Sc.)
In
SCHOOL OF PHYSICS AND MATERIAL SCIENCE

Submitted by

SIMRANJEET KAUR

ROLL No. 301004016

Under the guidance
of

Dr. POONAM UNIYAL

Assistant Professor

(School of Physics and Materials Science)

School of Physics and Materials Science

Thapar University, Patiala

Patiala (Punjab)-147001

June-2012

DEDICATED

TO

MY PARENTS

CERTIFICATE

This is to certify that the thesis entitled **"Synthesis and Characterization of Ce-doped Bismuth Ferrite"** *submitted by* **Ms. Simranjeet Kaur**, *Roll No.* **301004016** *in the partial fulfillment of the requirement for award of the degree of* **Master of science** , *from the* **School of Physics and Materials Science, Thapar University, Patiala,** *is record of candidate's own work carried out by her under my supervision and guidance. The matter embodied in this report has not been submitted in part or full to any other university or institute for the award of any degree.*

Poonam

(Dr. Poonam Uniyal)

Assistant Professor

School of physics and materials science

Thapar University

Patiala, Punjab

Countersigned By:

(Dr. Kulveer Singh)

Head and professor of Department of SPMS

Thapar University, Patiala

Punjab(147004)

(Dr. S K Mohapatra)

Dean of Academic Affairs

Thapar University, Patiala

Punjab(147004)

ACKNOWLEDGEMENT

First of all I would like to extend my deepest gratitude to my supervisor, **Dr. Poonam Uniyal** (Assistant Professor), School of Physics and Materials Science, Thapar University, Patiala, for giving me a chance to work in her supervision and without her help and constant guidance this thesis would have not completed. She steered me through this journey through her invaluable advice, positive criticism and consistent encouragement. Her attention towards my proceedings, her devoted time and her ideas has enabled me to make my thesis a success. Her faith in me has always made me more confident. Her blessing always made me optimistic.

I would also like to extend my thanks **Dr. K.L Yadav**, Assosiate Professor (I.I.T Roorkee), for his support, encouragement and assistance during my work. He has been very helpful in improving my dissertation. I am grateful to him for sharing his time and expertise. His comments and views were very insightful and helpful.

My sincere thanks to professor **K.K. Raina** for providing his lab facilities especially for di-electric measurements and also to his research scholar Ravi-Shukla who helped in taking measurements.

I am also grateful to Mrs. Nandini Sharma, Mintu tyagi PhD Scholars, School of Physics and Materials Science for their encouragement and execution of report work and providing me invaluable support and training in various techniques and uses of equipment.

I would also like to thank all the staff members of School of Physics and Materials Science for their support and encouragement.

I would also like to thank my parents for their all kind of support, encouragement and blessings. I am also very thankful to all my friends for their motivation and huge support.

Simranjeet Kaur

(Simranjeet Kaur)

Roll No. 301004016

CONTENTS

ABSTRACT

In the present work, we have studied the effect of Ce-doping on the structural and dielectric properties of $BiFeO_3$ ceramic. The phase characterization of $BiFeO_3$ is carried by X-ray Diffraction. The variation of dielectric constant and dielectric loss with temperature (40^0-500^0 C) in the frequency range of 100Hz-1 MHz is studied.

List of figures:

Chapter -1

Chapter-2

Chapter-3

List of tables:

Chapter -3

List of Symbols:

$BiFeO_3$	Bismuth ferrite
BCFO	Ce-doped Bismuth Ferrite
XRD	X-ray diffraction
SEM	Scanning electron microscope
ε	Dielectric constant
Tan(δ)	Tangent loss

CHAPTER-1

INTRODUCTION

1.1 THE CONCEPT OF MULTIFERROICS

1.1.1 History

Electricity and magnetism were combined into one common discipline in 19th century, culminating in the Maxwell equations. However, people used to think that ferroelectricity and magnetism are exclusive to each other and can only have weak coupling when they coexist. The term multiferroic was first used by H.Schmid in 1994[1]. His original definition referred to multiferroics as single phase materials which simultaneously possess two or more primary ferrroics properties. Today people extend the definition to include other long-range orders, such as antiferromagnetic. In this extended definition, we can say that this research field was born in the 1960's. From then people started to do related studies under the name magnetoelectric.

1.1.2 TYPES OF FERROICS [2]:

i. **Ferroelectric materials:** These materials possess a spontaneous polarization that is stable and can be suddenly switched hysteretically by an applied electric field.

ii. **Antiferroelectric materials:** These materials possess ordered dipole moments that cancel each other completely within each crystallographic unit cell.

iii. **Ferromagnetic materials:** These materials possess a spontaneous magnetization that is stable and can be switched hysteretically by an applied magnetic field;

iv. **Antiferromagnetic materials:** These materials possess ordered magnetic moments that cancel each other completely within each magnetic unit cell.

v. **Ferroelastic materials:** These materials display a spontaneous deformation that is stable and can be switched hysteretically by an applied stress.

vi. **Ferrotoroidic materials:** These materials possess a stable and spontaneous order parameter that is taken to be the curl of a magnetization or polarization. By analogy with the above examples, it is anticipated that this order parameter may be switchable.

vii. **Ferromagnetic materials:** These materials differ from antiferromagnets because the magnetic moment cancellation is incomplete in such a way that there is a net magnetization that can be switched by an applied magnetic field [2].

1.1.3 MULTIFERROICS AND MAGNETOELECTRICITY:

A single phase multiferroic material is one that possesses two or more ferroics properties i.e. ferroelectricity, ferromagnetism, ferroelasticity and ferrotoridicity. Generally current trend is to exclude the requirement for ferroelasticity property but to include the ferrotoroidic property. In a broader definition, antiferroic properties are also considered. The coupling between the magnetic and electric order has been known as magnetoelectric (ME) effect. Magnetoelectric coupling describes the coupling between magnetic and electric order parameters [2].

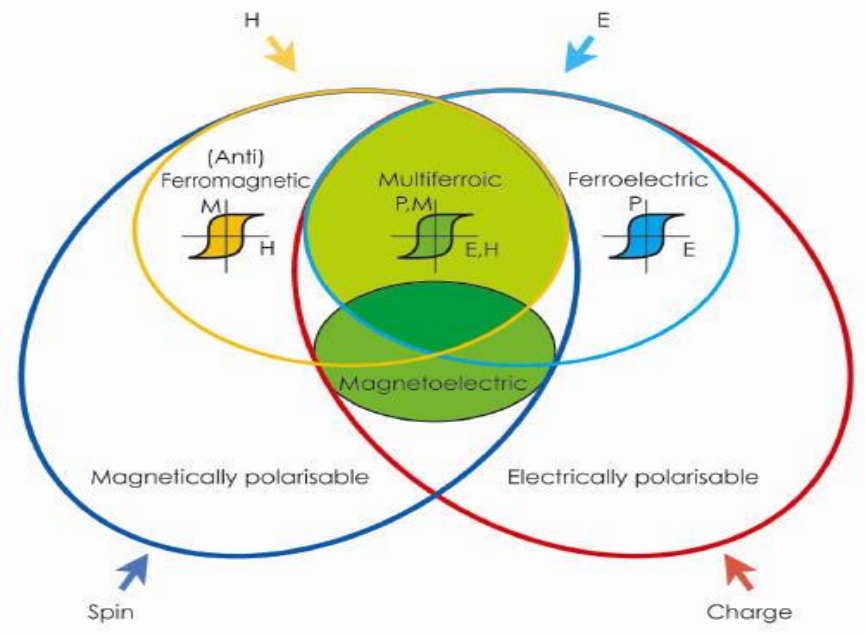

Figure 1.1 The intersection of two sets named magnetically and electrically polarizable material with subsets of ferromagnetic and ferroelectric called multiferroic and magnetoelectric effect.

The relationship between multiferroic and magnetoelectric is well reflected by figure-1.1. The figure describes that magnetically (electrically) polarizable materials form the subset of ferromagnetic (ferroelectric) materials. The intersection between them represents the multiferroic materials.Magnetoelectric coupling (green hatching) is an independent phenomenon that can, but need not, arise in any of the materials that are both magnetically and electrically polarizable.

1.1.4 ORDER PARAMETER COUPLING:

i. **Magnetoelectric coupling:** It describes the influence of a magnetic (electric) field on the polarization (magnetization) of a material.
ii. **Piezoelectricity:** It describes a change in strain as a linear function of applied electric field, or a change in polarization as a linear function of applied stress.
iii. **Piezomagnetism:** It describes a change in strain as a linear function of applied magnetic field, or a change in magnetization as a linear function of applied stress.
iv. **Electrostriction:** It describes a change in strain as a quadratic function of applied electric field.
v. **Magnetostriction:** It describes a change in strain as a quadratic function of applied magnetic field [2].

1.1.5 CLASSIFIACTION OF MULTIFERROICS:

1.1.5.1 Charge order multiferroics

Charge ordering can occur in compounds containing ions of mixed valence with geometrical or magnetic frustration. A famous example is $LuFe_2O_4$, the ordering of Fe^{2+} and Fe^{3+} provides ferroelectricity below 330K and ferromagnetic behaviour occurs below 240K [3].

1.1.5.2 Geometerically frustrated multiferroics

Geometrical multiferroic is another type. The mechanism of ferroelectricity is considered as nonlinear couplings between different lattice distortions, suggested by first principle calculations. A proper example of this compound would be hexagonal $RMnO_3$, in which the coupling of different phonon modes creates ferroelectricity. Geometrical reasons also produce magnetically induced ferroelectricity [4].

-

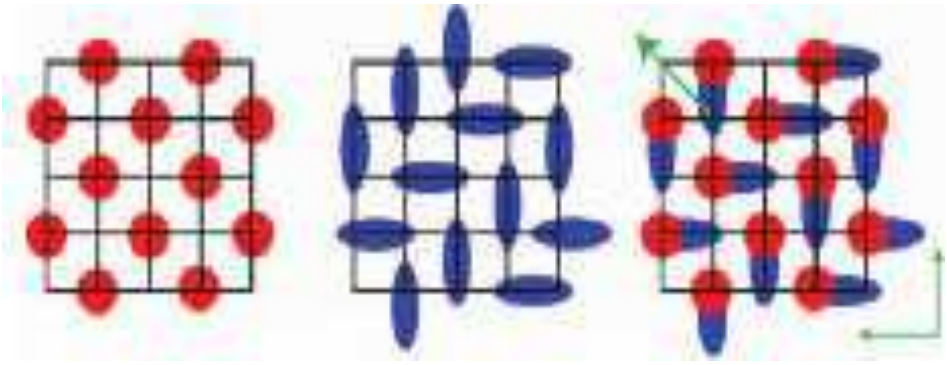

Figure.1.2: Left: site-centred charge ordering. Mid: bond-centred charge ordering. Right: ferroelectricity by Charge Ordering. This picture is taken from ref.5.

1.1.5.3 Lone pair multiferroics

In usual perovskite-based ferroelectrics like $BaTiO_3$, the ferroelectric distortion occurs due to the displacement of B-site cation (Ti in $BaTiO_3$) with respect to the oxygen octahedral cage. Here the transition metal ion (Ti in $BaTiO_3$) requires an empty "d" shell since the ferroelectric displacement occurs due to the hybridization between Ti "3d" states and O "2p" states. This normally excludes any net magnetic moment because magnetism requires partially filled "d" shells. However, partially filled "d" shell on the B-site reduces the tendency of perovskites to display ferroelectricity In order for the coexistence of magnetism and ferroelectricity (multiferroic), one possible mechanism is lone-pair driven where the A-site drives the displacement and partially filled "d" shell on the B-site contributes to the magnetism. Examples include $BiFeO_3$, $BiMnO_3$, $PbVO_3$ [6].

1.1.5.4 Magnetically driven ferroelectric multiferroics

Magnetically driven multiferroics are insulating materials, mostly oxides, in which macroscopic electric polarization is induced by magnetic long range order. A necessary but not sufficient condition for the appearance of spontaneous electric polarization is the absence of inversion symmetry. In these materials inversion symmetry is broken by magnetic ordering. Such a symmetry breaking often occurs in

so called frustrated magnets, where competing interactions between spins favour un conventional magnetic order [7]. The microscopic mechanisms of magnetically induced ferroelectricity involve the polarization of electronic orbitals and relative displacement of ions in response to magnetic ordering.

1.1.6 Why multiferroic is a rare phenomenon??

By definition, for a material to be magnetoelectric multiferroic, it must be simultaneously ferromagnetic and ferroelectric. Therefore, it's allowed physical, structural and electronic properties are restricted to those which occur both in ferromagnetic and in ferroelectric materials. In this section, we analyze a range of properties and discuss how these limit our choice of potential multiferroic materials [8].

Generally ferroelectricity is produced by vacant d^0 orbital and ferromagnetism is observed due to partially filled d^n orbital.

1.1.6.1 Chemistry of d^0 subshell:

The common perovskite oxide ferroelectric materials have a formal charge corresponding to the d^0 electron configuration on the B cation. It is clear, if there are no d electron of any type creating localized magnetic moment, then there can be no magnetic ordering of any type, either ferro, ferri, or antiferromagnetic. It appears however that, in most cases, as soon as the d shell on the small cations is partially occupied, tendency for it to make a distortion that removes the center of symmetry is eliminated. This could be the result of a number of effects, including size, the tendency to undergo a different, more dominant distortion, electronic properties, magnetic properties [9].

1.1.6.3 Size of small cations:

The transition metal ions with occupied d shells are simply too large to move away from the large space at the center of the oxygen octahedron. In this section, we compare the ionic radii of typical d^0 cations in perovskite ferroelectrics with those of typical d^n cations in nano ferroelectric perovskite oxides to see if this argument is correct, The Shannon ionic radii of some common d^o small cations found in

ferroelectric perovskite oxides are: Ti^{4+}= 74.5 pm, Nb=78 pm , and Zr=86 pm. Some representative d^n cations that are found as the small cations in non ferroelectric perovskite oxides include $Mn^{3+}(d^4)$ with $Ti^{3+}(d^1)$and $V^{4+}(d^1)$ with radii of 78.5pm, 81pm and 72pm respectively. Therefore, typical B-site cations with d electron occupation do not have systematically larger radii than typical d^0 B-site cations. The size of the B cations is not the deciding factor in the existence or otherwise of ferroelectricity [9].

1.1.7 EXAMPLES OF MULTIFERROICS

Typical multiferroics belong to the group of the perovskite (Fig.1.3) transition metal oxides and include rare-earth magnetites and ferrites such as $TbMnO_3$, YMn_2O_5 and $LuFe_2O_4$. Other examples are the bismuth compounds $BiFeO_3$, $BiMnO_3$ and non-oxides such as $BaNiF_4$.

1.1.8 GENERAL PERVOSKITE STRUCTURE

The general chemical formula for perovskite compounds is ABX_3, where 'A' and 'B' are two cations of different sizes, and X is an anion that bonds to both. The 'A' atoms are larger than the 'B' atoms. The ideal pervoskite structure has the B cations in 6-fold coordination, surrounded by an octahedron of anions, and the A cation in 12-fold cuboctahedral coordination. The relative ion size requirements for stability of the cubic structure are quite stringent, so slight buckling and distortion can produce several lower-symmetry distorted versions, in which the coordination numbers of A cations, B cations or both are reduced.

Yellow spheres are X atoms –usually oxygen.

Deep blue spheres are A-site atoms-usually a larger metal cations.

Green sphere is B-site atoms-usually smaller metal cation.

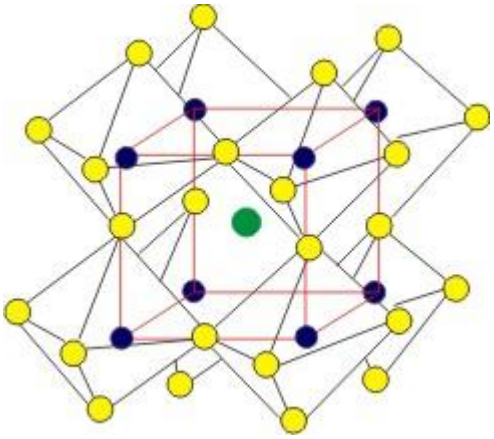

Figure: 1.3 General Perovskite structure

1.2 BISMUTH FERRITE

1.2.1 Introduction to $BiFeO_3$:

$BiFeO_3$ (BFO) is an inorganic chemical compound with a perovskite structure. It is one of the most promising lead-free piezoelectric materials by exhibiting multiferroic properties at room temperature. Multiferroic materials exhibit ferroelectric or antiferroelectric properties in combination with ferromagnetic (or antiferromagnetic) properties in the same phase. $BiFeO_3$ is the only prototype among all other multiferroic oxides which shows both ferromagnetism and ferroelectricity in a single crystal above room temperature. It has ferroelectric Curie temperature T_c = 1143K and antiferromagnetic Neèl temperature T_N = 643K. The ions responsible for the production of ferroelectricity and magnetism are Bi^{3+} and Fe^{3+} ions. Ferroelectricity is produced due to Bi^{3+} and antiferromagnetism is due to Fe^{3+} ions [2].

1.2.2 Crystal structure of $BiFeO_3$:

- It is having rhombohedrally distorted perovskite structure with R3c space group at room temperature.

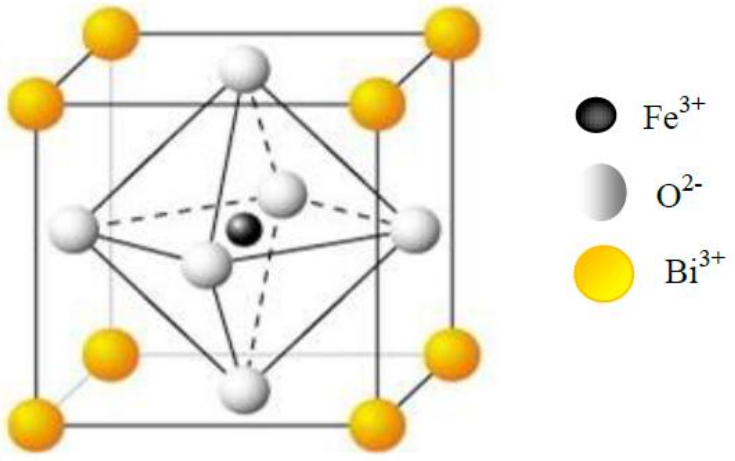

Fig 1.4 $BiFeO_3$ in Perovskite structure

- Bi^{3+} ion occupy the corner position, Fe^{3+} in the body centered position, and O^{2-} in all face centered position. The lattice parameters are a = 5.587 Å, b = 5.587 Å and c = 13.867 Å with $\alpha = \beta = 90^0$ and $\gamma = 120^0$. The hexagonal unit cell contains 6 units.

  Generally ferroelectricity is produced by vacant d^0 orbital and ferromagnetism is observed due to partially filled d^n orbital. In $BiFeO_3$, ferroelectricity is produced due to stereo chemical activity of Bi^{3+} ion and ferromagnetism is due to Fe^{3+} ions [2].

- **Production of ferroelectricity in bismuth ferrite:**
  Bi^{3+} and Fe^{3+} cations displaced along the [1 1 1] three fold polar axis and off centered with respect to the body centre of the oxygen octahedron, which in turn gives rise to ferroelectricity.

- **Production of ferromagnetism in bismuth ferrite:**
  It is produced due to rotations of adjacent oxygen FeO_6 octahedral around the [1 1 1] pseudo cubic direction (figure-1.4).

1.2.3 Applications of $BiFeO_3$ [2]:

1. Due to multiferroic nature of $BiFeO_3$ it has broader applications in the field of transducers, magnetic field sensors and information storage industry.

2. Due to its magnetoelectric coupling it has the advantage that data can be written electrically and read magnetically. It exploits the best aspects of ferroelectric random access memory (FeRAM) and magnetic data storage. Multiferroism leads to fast, low-power consumption, multifunctional memory devices exploiting the best attributes of conventional ferroelectric and magnetic random-access memories.

3. Recently, ferroelectric random access memories (FeRAMs) have achieved fast access speeds (5 ns), high densities (64 Mb).

1.3 LITERATURE REVIEW:

Incorporation of $BiFeO_3$ into practical device application has been leakage problems that lead to low resistivity-presumably basically due to the defects and also due to impurities and non-stoichiometery related issues (Vaz et al. 2010,Hu et al. 2008). $BiFeO_3$ also cannot be exploited for the device applications due to other major problems such as week magnetization, it being essentially an anti-ferromagnetic below temperature $T_{N,}$ large loss factors because of oxygen non-stoichiometery, low-magnetoelectric coupling (P.Uniyal 2009).

To overcome these problems, a number of studies on different parameters such as A or B site substitution and co-doping has been investigated, this results in lowering the leakage current and increasing the resistance by eliminating secondary impurities oxygen vacancies thereby improving ferroelectric properties.

Doped multiferroics offer an exciting expansion to this list. Improvement in multiferroic properties of $BiFeO_3$ was found $BiFeO_3$ after doping it with different alkaline-earth metal ions. Introduction of rare earth ions at A site of $BiFeO_3$, particularly La-doped $BiFeO_3$ also show favorable results. Cerium a rare earth element, despite having similar ionic radius as Bi has attracted less attention of the

researches to work with. Wang et al. have reported substantially enhanced electric and dielectric properties in Ce-doped $BiFeO_3$ thin films grown on $LaNiO_3$/Si substrate using the sol-gel method. Ce doping has also been shown to reduce the leakage current density in $BiFeO_3$ thin films.

CHAPTER-2

EXPERIMENTAL TECHNIQUES

2.1 EXPERIMENTAL TECHNIQUES

The characterization of materials regarding determination of electrical composition, estimation of trace impurities, structural analysis, morphological analysis, dielectric analysis, identification of crystalline phases and information on crystal defects play an important role for the quality control and development of advanced materials and their use in precision devices. For the $BiFeO_3$, characterization techniques include

- X-ray diffraction (XRD)
- Scanning Electron Microscopy (SEM)
- Di-electric measurement (LCR Bridge)

2.1.1 X-ray diffraction (XRD)

Single-crystal X-ray Diffraction is a non-destructive analytical technique which provides information about the atomic spacing of crystalline substances, including unit cell dimensions, bond-lengths, bond-angles, and details of site-ordering. The data generated from the X-ray analysis is interpreted and refined to obtain the crystal structure.

Principle of X-ray Diffraction

One of the best method of determining a crystal's structure and atomic spacing is by X-ray diffraction. In X-ray diffraction experiments, an intense beam of X-ray strikes the crystal of study. In general, crystal diffracts the X-ray beam differently, depending on its structure and orientation. The diffracted X-ray is collected by an area detector. The diffraction pattern consists of reflections of different intensities which can be used to determine the structure of the crystal. However, many different orientations of the crystal need to be collected before the true structure of the crystal can be determined.

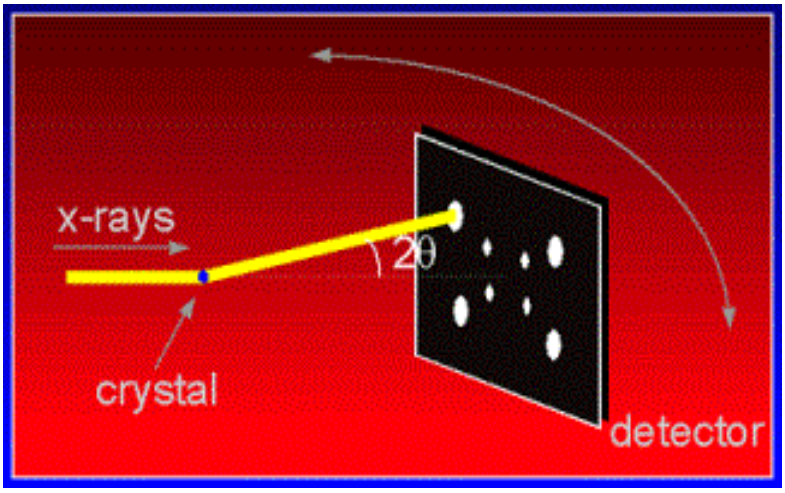

Figure: 2.1 X-ray Diffraction

The resolution of an X-ray diffraction detector is determined by the Bragg equation:

$$d = \frac{1}{2}\left(\frac{\lambda}{\sin\theta}\right)$$

Where d is the resolution of the detector, λ is the incident x-ray wavelength, and θ is the angle of diffraction.

2.1.2 Scanning electron microscope (SEM):

A scanning electron microscope (SEM) is a type of electron microscope that images a sample by scanning it with a high-energy beam of electrons in a raster scan pattern. The electrons interact with the atoms that make up the sample producing signals that contain information about the sample's surface topography, composition, and other properties such as electrical conductivity etc.

Figure: 2.2 SEM chamber

Working of scanning electron microscope:

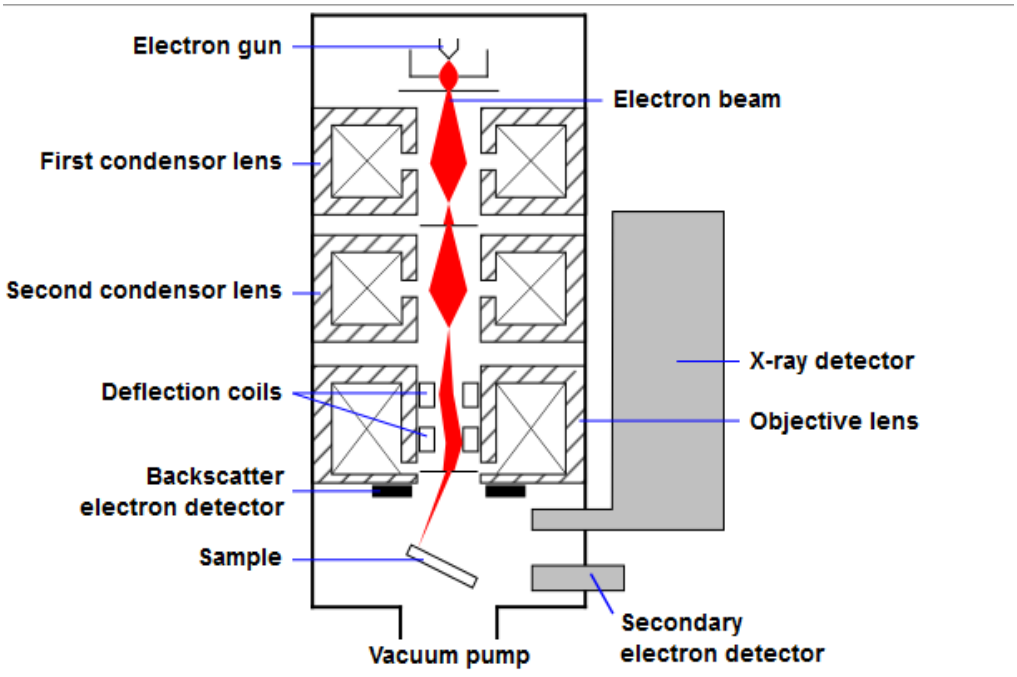

:

Figure: 2.3 Schematic diagram of a SEM.

In a typical SEM, an electron beam is thermionically emitted from an electron gun fitted with a tungsten filament cathode. Tungsten is normally used in thermionic electron guns because it has the highest melting point and lowest vapour pressure of all metals, thereby allowing it to be heated for electron emission, and because of its lower cost.

The electron beam, which typically has an energy ranging from 0.2 keV to 40 keV, is focused by one or two condenser lenses to a spot about 0.4 nm to 5 nm in diameter. The beam passes through pairs of scanning coils or pairs of deflector plates in the electron column, typically in the final lens, which deflect the beam in the *x* and *y* axes so that it scans in a raster fashion over a rectangular area of the sample surface.

When the primary electron beam interacts with the sample, the electrons lose energy by repeated random scattering and absorption within a teardrop-shaped volume of the specimen known as the interaction volume, which extends from less than 100 nm to around 5 µm into the surface. The size of the interaction volume depends on the electron's landing energy, the atomic number of the specimen and the specimen's density. The energy exchange between the electron beam and the sample results in the reflection of high-energy electrons by elastic scattering, emission of secondary electrons by inelastic scattering and the emission of electromagnetic radiation, each of which can be detected by specialized detectors. The beam current absorbed by the sample can also be detected and used to create images of the distribution of specimen current. Electronic amplifiers of various types are used to amplify the signals, which are displayed as variations in brightness on a cathode ray tube. The raster scanning of the Cathode ray tube (CRT) display is coordinated with that of the beam on the sample in the microscope, and the resulting image is therefore a distribution map of the intensity of the signal being emitted from the scanned area of the sample. The image can be captured by photography from a high-resolution cathode ray tube (CRT), but in modern machines it is digitally captured and displayed on a computer monitor and saved to a computer's hard disk.

2.1.3 Dielectric Measurement

To measure the dielectric constant and dielectric loss, LCR (HIOKI model 3532-50) meter was used. In this work, LCR (HIOKI model 3532-50) Tester was used to measure the dielectric constant and dielectric loss. The electroded samples were used to take the measurements. The LCR meter, was interfaced with the computer and the data (capacitance and *D* factor) was collected as a function of temperature at different frequencies. The measured capacitance was then converted into dielectric constant using the following formula:

$C=\varepsilon_0\varepsilon_r A/d$

where, *C* : Capacitance in farad (*F*)

ε_0 : Permittivity of free space in farad per meter ($8.85 \times 10^{-12} F/m$)

ε_r : Dielectric constant or relative permittivity of the sample.

A : Area of each plane electrode in square meters (m^2)

d : Separation between the electrodes in meters (*m*)

The study of dielectric properties is concerned with the storage and dissipation of electric and magnetic energy in materials. A dielectric material is a substance that is a poor performer of electricity, but an efficient supporter of electrostatic fields. If the flow of current between opposite electric charge poles is kept to a minimum while the electrostatic lines of flux are not interrupted or impeded, an electrostatic field can store energy. This property is useful in capacitors, especially at particular frequencies (radio frequencies). Dielectric materials are also used in the construction of radio-frequency transmission lines

CHAPTER-3

RESULTS AND DISSCUSION

MATERIALS AND METHOD

3.1 Synthesis of Bismuth ferrite

The $Bi_{1-x}Ce_xFeO_3$ (x=0.0 and 0.1) samples were prepared by a standard solid state reaction method using Bi_2O_3 (LOBA Chemicals, India), Fe_2O_3 (LOBA Chemicals, India) as a starting materials. Firstly the Bi_2O_3, Fe_2O_3 and CeO_2 in stoichiometery ratios were thoroughly mixed in proper stoichiometric ratios for 4-5 hrs. The mixture was calcined at 800^0 C for 2 hrs and then powder was ground and cold pressed into pellets and sintered at 820^0 C for 2 hrs. Finally these pellets were used for further characterizations and measurements.

3.2 RESULTS AND DISSCUSION:

3.2.1 X-ray Diffraction

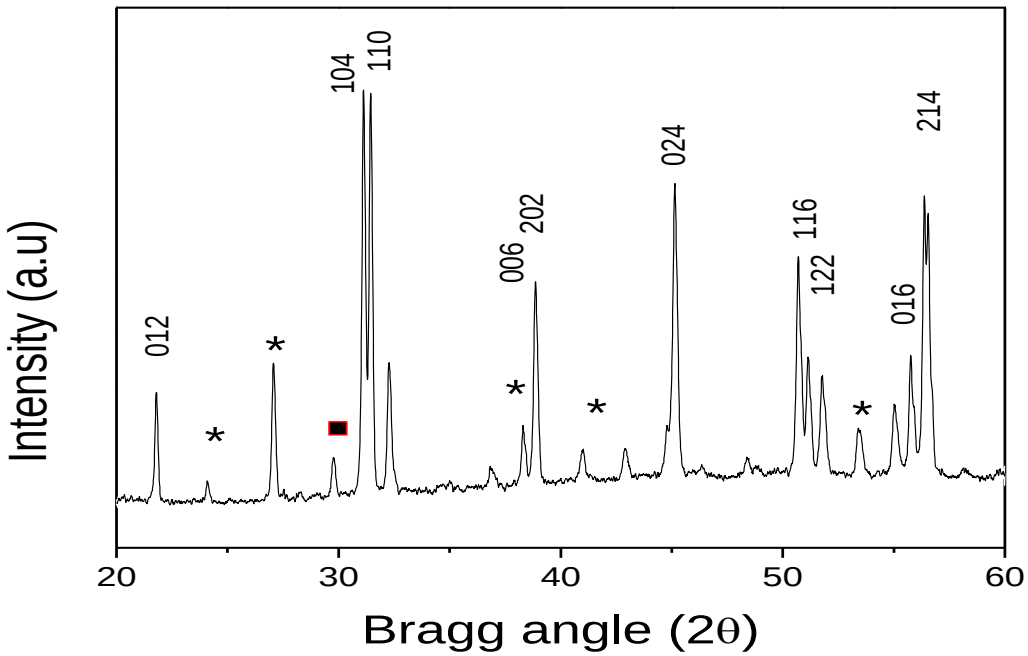

Figure:3.1 XRD Spectra of $BiFeO_3$ [* $Bi_{24}FeO_{40}$/ □$Bi_2Fe_4O_9$]

The XRD pattern obtained for BFO ceramics is shown in the Fig. 3.1 Preparation of phase-pure $BiFeO_3$ is reported to be difficult because of its narrow temperature range of phase stabilization. Various impurity phases have been reported to occur, mainly comprising of $Bi_2Fe_4O_9$, $Bi_{12}(Bi_{0.5}Fe_{0.5})O_{19..5}$ and $Bi_{25}FeO_{40}$, since $BiFeO_3$ is metastable with respect to $Bi_2Fe_4O_9$ (mullite phase) and $Bi_{25}FeO_{39}$ (sillenite phase). It is widely accepted that the presence of these impurities results in high leakage current in $BiFeO_3$ and poor ferroelectric behavior and thus render this material unsuitable for practical applications [20,21]

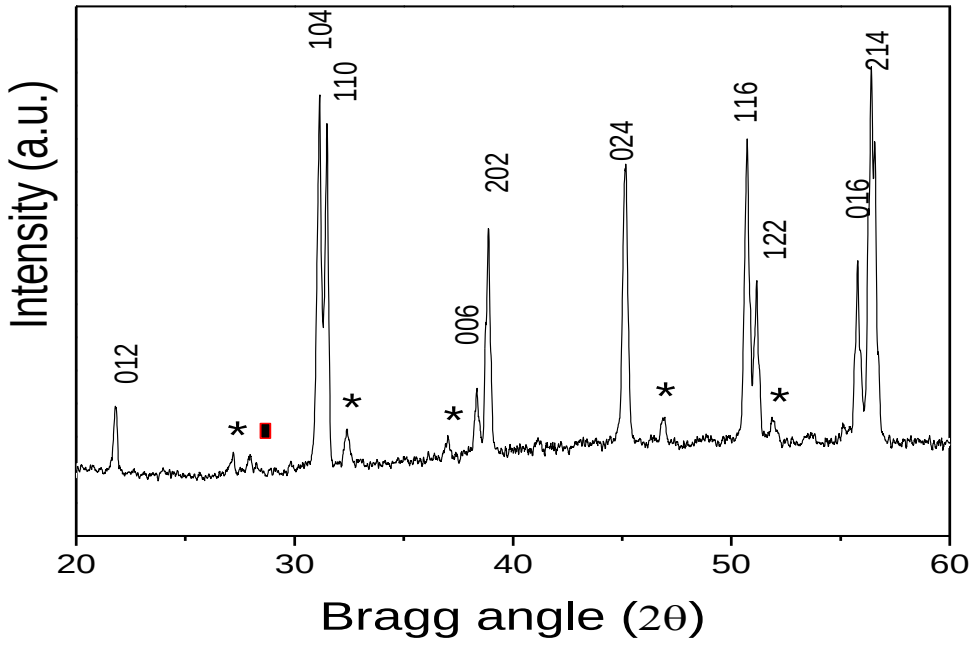

Figure:3.2 XRD Spectra of $Bi_{0.90}Ce_{0.10}FeO_3$ [* $Bi_{24}FeO_{40}$/ □$Bi_2Fe_4O_9$]

XRD pattern obtained for $Bi_{0.90}Ce_{0.10}FeO_3$ ceramics is shown in the Fig. 3.2. The XRD pattern for the annealed sample reveal the characteristic well crystallized pattern as that of pure $BiFeO_3$ along with some impurity phases which are always obtained along with $BiFeO_3$ as the minor phase due to chemical kinetics of formation. Ce^{3+} ions substitution for Bi in $BiFeO_3$ has not affected the structure of the parent compound. The intensity of impurity peaks is reduced with the increase in Ce^{3+} ion concentration. The elimination of secondary phase in Ce doped $BiFeO_3$ samples is a consequence of Ce doping. The lattice parameters are found to increase with Ce doping because ionic radii of Ce^{3+} is more than that of Bi^{3+} ion and the values are given in the table 3.1.

Table:3.1 The values of Lattice parameters (‘a’ and ‘c’)

Value of ‘x’	Lattice Parameter (a) (Å)	Lattice Parameter (c) (Å)
0.0(pure BFO)	5.352(1)	13.421(3)
0.1 (Doped BFO)	5.635(3)	13.678(4)

3.2.2 Microstructural analysis

Figure 3.3 and 3.4 shows the SEM micrographs of BFO and BCFO ceramics respectively. The microstructure of the sintered pellets of BFO show randomly oriented grains. A small amount of porosity is also evident from the micrograph. Ceramic with $x = 0.05$ shows a fine grained structure with sharp grain boundaries.

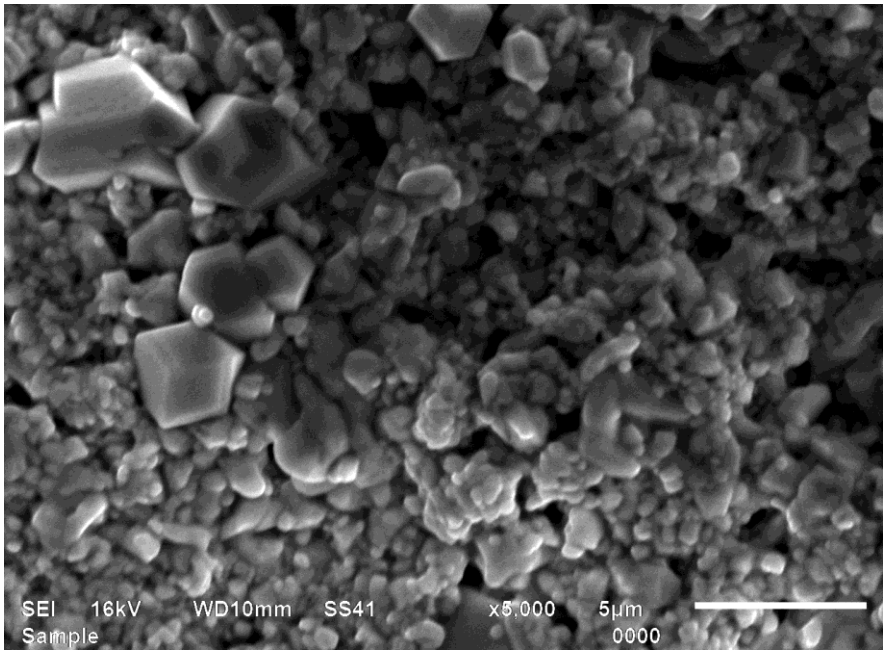

Figure: 3.3 Scanning electron micrographs of $BiFeO_3$ ceramic.

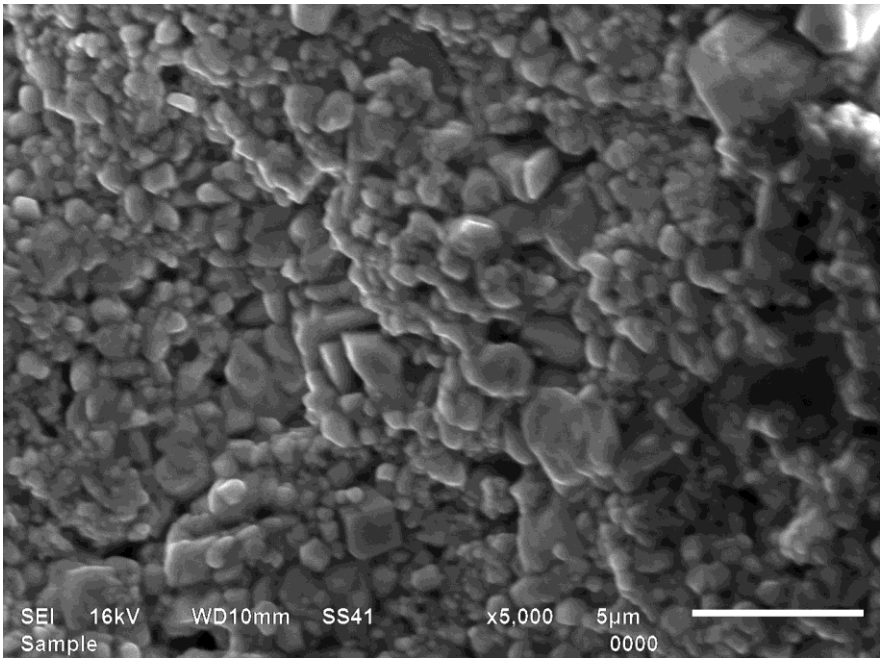

Figure:3.4 Scanning electron micrographs of $Bi_{0.90}Ce_{0.10}FeO_3$ ceramic.

3.2.3 Dielectric studies

The frequency dependence of dielectric constant (ε) and dielectric loss (tan δ) of $BiFeO_3$ and $Bi_{0.90}Ce_{0.10}FeO_3$ samples at room temperature have been shown in Fig. 3.5-3.6 respectively.

The mechanism of variation of dielectric constant of the ceramic with frequency can be explained in terms of four types of polarizations which contribute to the dielectric constant of the materials. These are: electronic, ionic, orientation and space charge polarizations. In the frequency range of 10^2 Hz to 10^4 Hz both ε and tanδ were found to decrease with increase in frequency. Generally both of these parameters decrease with increase in frequency and hence show a typical characteristic of dielectrics (ferroelectrics). In this audible range of frequencies all the polarizations are present, but the space charge polarization is prominent as per the theory of dielectric polarization. The space charge contribution depends upon the purity and perfection of the crystals and exhibits itself prominently at low frequencies and is purely surface effect phenomenon. Increase in the space charge phenomenon of solid increases the value of ε and tanδ. This polarization arises due to defects and impurities present

either in the bulk or at the surface of the crystal or both. As the frequency is increased beyond 10 kHz, both ε and tan δ become almost constant. Initial decrease in ε and tanδ with frequency (up to 100 kHz) can be explained by the phenomenon of dipole relaxation where in at low frequencies the defects related dipoles are able to follow the frequency of the applied field providing high values of ε, but begin to lag behind the field with increasing frequency[25]

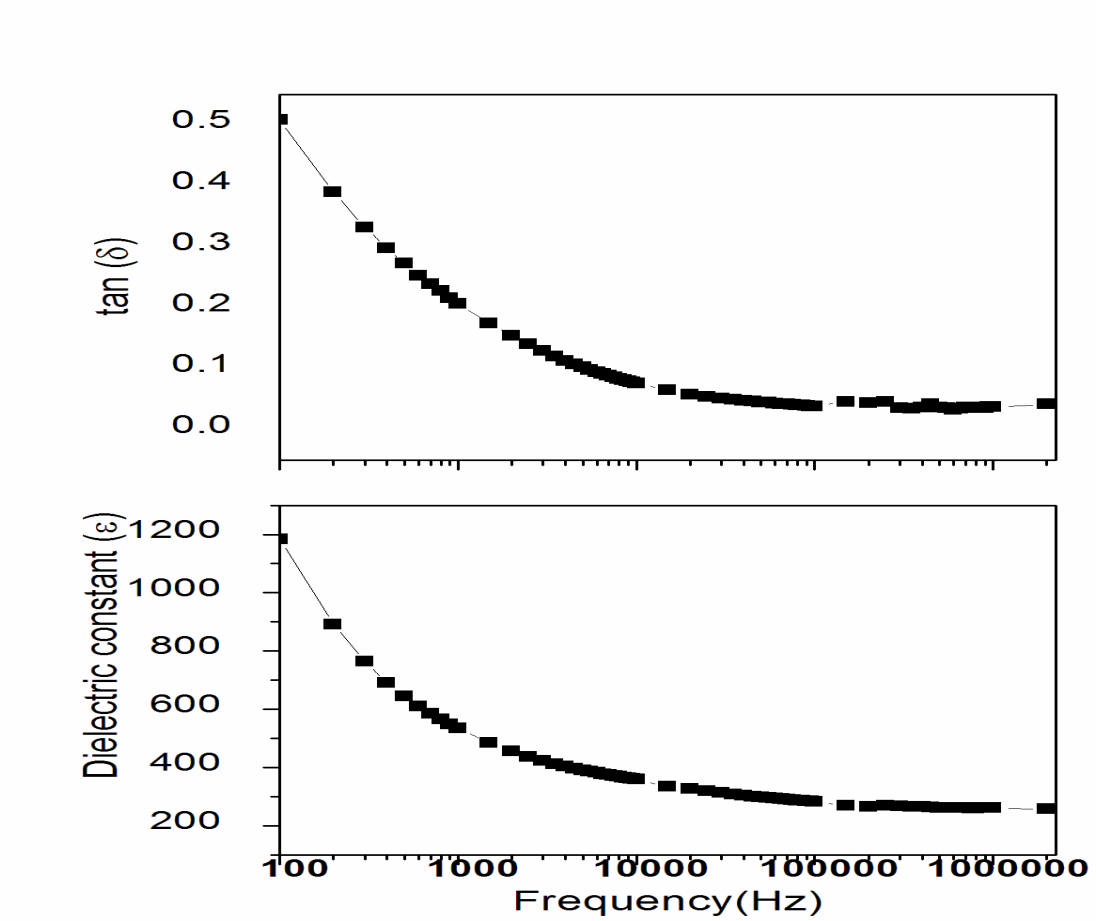

Figure:3.5 Variation of dielectric loss and dielectric constant with frequency for $BiFeO_3$ ceramic.

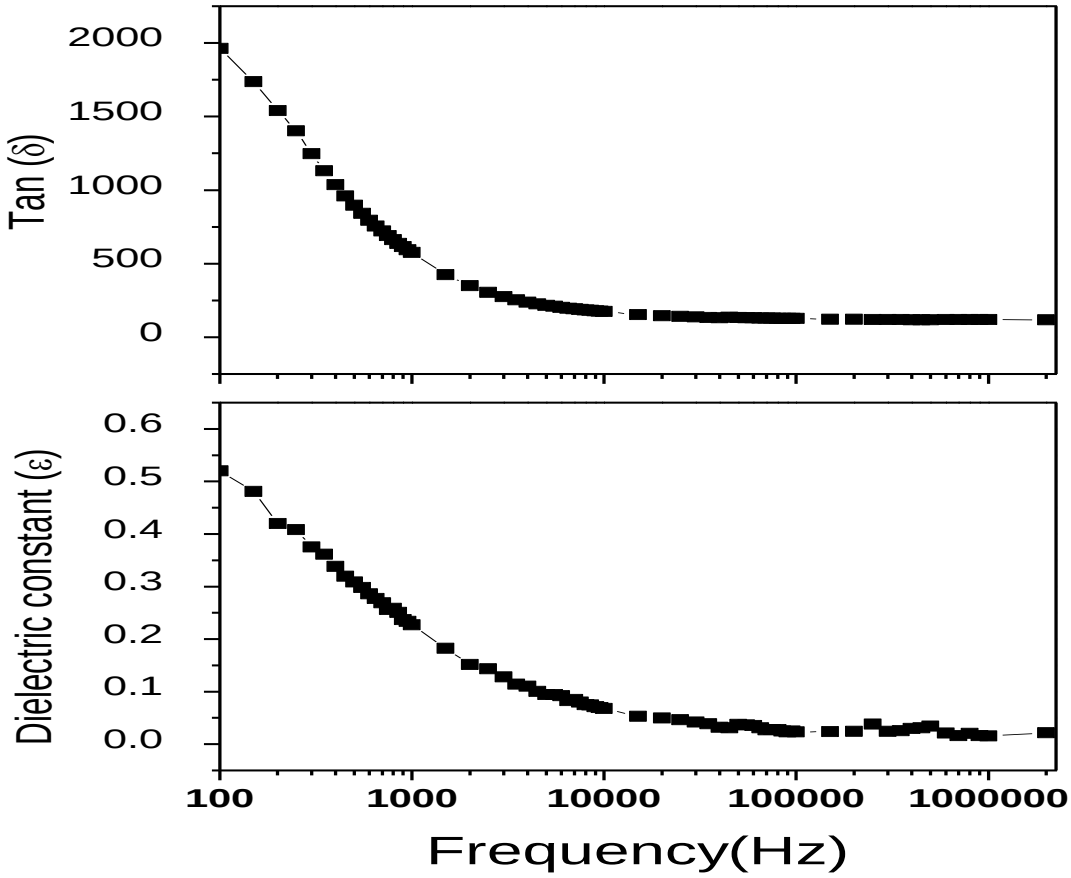

Figure:3.6 Variation of dielectric loss and dielectric constant with frequency for Ce-doped $BiFeO_3$ ceramic.

Figure 3.5-3.6 shows the temperature dependence of dielectric constant (ε) at various frequencies of the $BiFeO_3$ (BFO). The dielectric constant increases with increase in temperature upto a critical value which is near antiferromagnetic Néel temperature (T_N). The T_N value is found to be frequency dependent. It shifts from 400 ^oC at 1 kHz to 415^oC at 100 KHz on increasing the measuring frequency, with a concomitant decrease in the peak value of dielectric constant, mimicking a relaxor ferroelectric behavior. Very high value of ε of the order of 10^4 is indicative of highly conducting nature. Since nonstoichiometric oxygen deficiency is an inherent problem with $BiFeO_3$. So, there is always some contribution of space charge polarization due to oxygen ion vacancies in the entire temperature range. But at higher temperature this effect becomes more prominent due to thermally activated process, for which the tanδ value shoots up to very high value as shown in Figure 3.8[23,24]

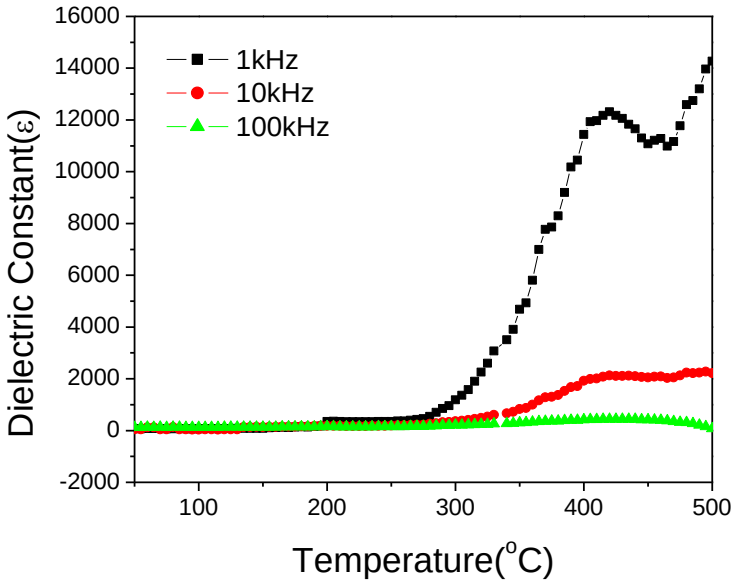

Figure:3.7:Variation of dielectric constant of $BiFeO_3$ ceramic with temperature at different frequencies

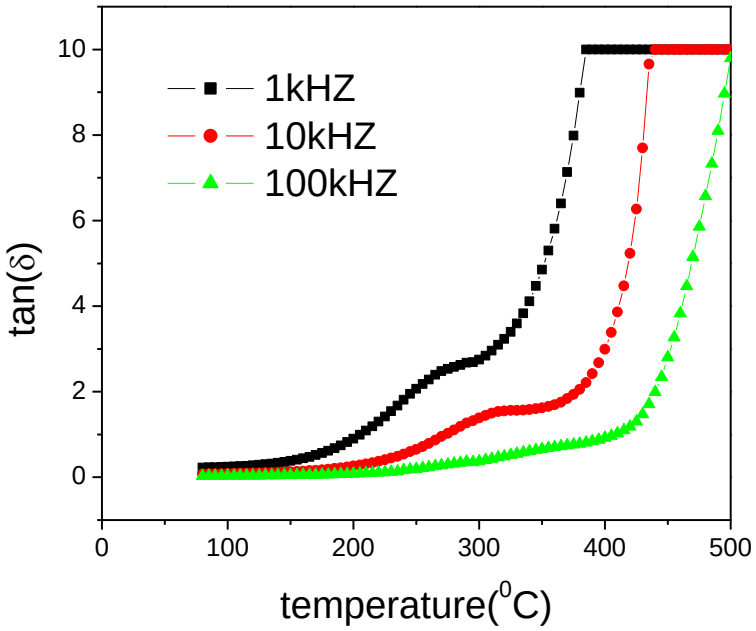

Figure:3.8 Variation of tangent loss of $BiFeO_3$ ceramic with temperature at different frequencies

Similar behaviour of dielectric constant and dielectric loss is observed for Ce- doped $BiFeO_3$ as shown in Figure 3.9and 3.10.

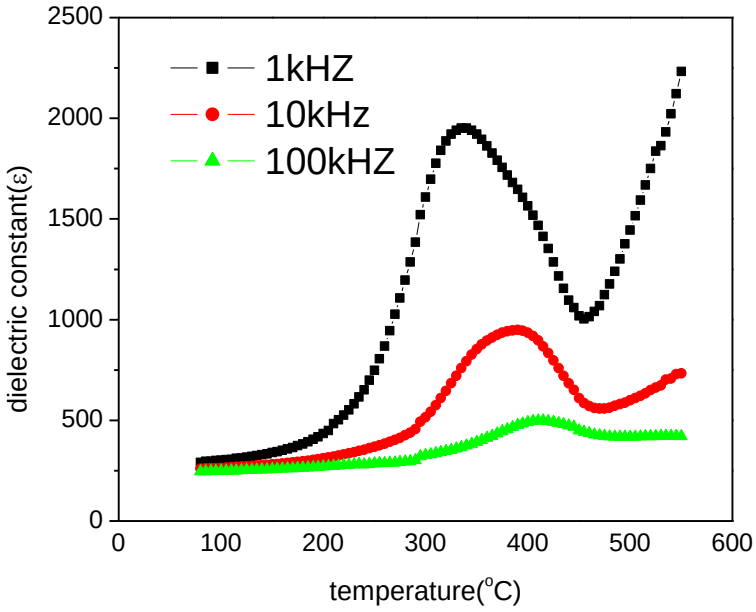

Figure:3.9 Variation of Dielectric constant of Ce-Doped $BiFeO_3$ with temperature at different frequencies

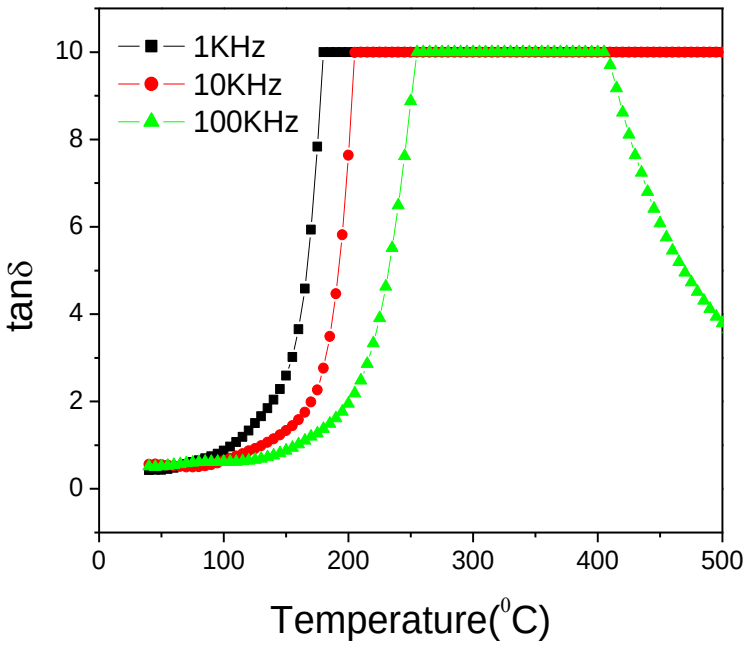

Figure:3.10 Variation of tangent loss of Ce-Doped $BiFeO_3$ with temperature at different frequencies.

Observation of dielectric anomaly near antiferromagnetic temperature is an evidence of magnetoelectric coupling in the system. The T_N is shifted to lower value with the Ce doping.

CHAPTER -4

CONCLUSIONS

4.1 CONCLUSIONS AND FUTURE SCOPE

In the present study, $Bi_{1-x}Ce_x FeO_3$ (x=0, 0.1) ceramics were prepared by solid state reaction method. Structural characterizations of all the synthesized samples were done with X-ray diffractometer. Ce substitution at a Bi site reduced the usual impurity phase in $BiFeO_3$ and stabilized the crystal structure.

Dispersion in dielectric constant and dielectric loss at lower frequencies was observed. An anomaly in the dielectric constant in the vicinity of the antiferromagnetic Neèl temperature (T_N) was observed, which is a signature of magnetoelectric coupling.

The present work is only aimed to study the dielectric behavior of the synthesized compounds. One may further do the detailed study of the magnetic and ferroelectric behavior of this Ce doped $BiFeO_3$ system in future.

References

1. H. Schmid, Ferroelectrics 162, 317 (1994).
2. J.F.Scott, Nature Reviews 442, 759 (2009).
3. N.Ikeda, H.Ohsumi, K.Ohwad, K.Ishii, T.Inam, K.Kakurai, Y.Murakami, S.Mori, Y.Horibe, H.Kito, Nature 436 (7054), 1136 (2005).
4. C. J. Fennie, K.M. Rabe, Physical Review 72,100103 (2005).
5. D.V. Efremov, J. V. Brink, D.I. Khomskii, Nature materials 3, 853 (2004).
6. A. J. Hatt and N. A. Spaldin, Eur. Phys. 71, 435 (2009)
7. T.Kimura, G.Lawes, A.P Ramirez, and Y.Tokura. Phys. Review 92, 257201 (2004).
8. N. A. Hill, Annual Review of Materials Research 32, 1 (2002).
9. N.A Hill, Phys.Chem.104,29 (2004)
10. W. Eerenstein, N.D Mathur & J.F Scott, nature,442,759(2006).
11. N. Lebeugle , Nature Reviews Physical Review 76, 024116 (2007)
12. C.P. Bhole Archives of Applied Science Research 3, 384-389 (2011)
13. JM. Harp, DE .Timm, GJ. Bunick Acta crystallographic 54,622–9761858 (1998).
14. S,Foner, Rev.sci. Instrum 30, 548(2004).
15. F. Kubel, H. Schmid, Acta Cryst. 46, 698(1998).
16. a) E. Ascher, J. Phys. C: Solid State Physics 10,1365. b) M. V. Jaric, D.Mukamel, Nucl. Phys.336, 475(1997).
17. T. T. Carvalho, European Summer School of Multiferroics, Girona 56, 3434(2008).
18. J. Privratska, V. Janovec, Ferroelectrics 204, 321(1997).
19. D. H. Kim, H. N. Lee, M. D. Biegalski, H. M. Christen, Appl. Phys. 34, 012911 (2008).
20. T J, Reague, R, Gerson and JW, James, Solid State Commun. 32, 81073 (1999).
21. R K .Mishra, D K .Pradhan, R N P. Chaudhary and A J. Banerjee. Phys.: Condens. Matter 20 ,045218 (2008).
22. S. R.Shannigrahi, A.Huang, D.Tripathy, A.O.Adeyeye, J.Magn. Mag.Maters.320, 221 (2008).
23. X. Zhang,Z. Wen, X. Lang, D.Wu, T.Qiu, M. X.Xu, J. Ally. Compds., 499,108 (2010)

24. V A.Khomchenko, D A. Kiselev, EK. Selezneva, J M.Vieira, A. M. L. Lopes, 320 5152 (2001) .
25. P.Uniyal, K.L. Yadav Mater Lett 62 ,2858 (2008).
26. M. Fiebig, J. Physics 38, 123 (2005).
27. G. A. Smolenskii, I. E. Chupis J.physics 137, 415 (2000).
28. J.R. Cheng, N. Li, and L. E. Cross, J. Appl. Phys 94,5153 (2003)
29. M. Kumar, K. L.Yadav, and G. D. Varma, Mater. Lett 62, 1159 (2008).
30. V R.Singh, A. Dixit, A.Garg, and D C.Agrawal, Appl. Phys. A:Mater. Sci. Process 90, 197 (2008).
31. N. A. Spaldin and M. Fiebig, Review Science 309,391 (2005)